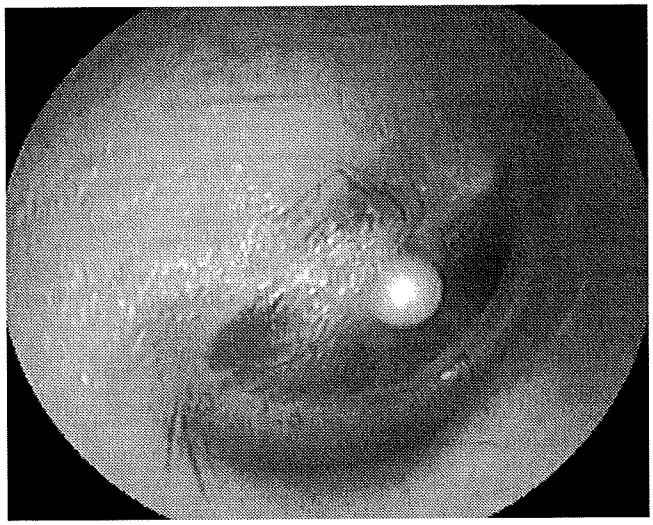

Fig. 1. Intratympanic membrane congenital cholesteatoma in Case 1.

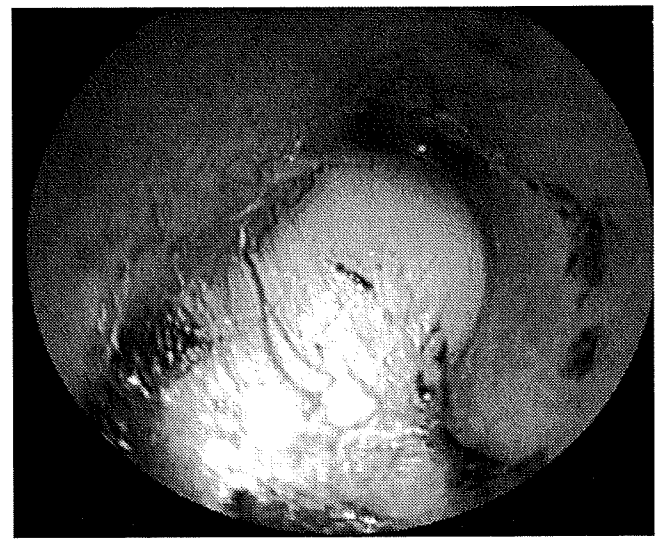

Fig. 3. Intratympanic membrane congenital cholesteatoma in Case 2.

ear was healing well with no recurrence (Fig. 5) and an audiogram showed a 10-dB conductive hearing loss on the right side compared to the left side.

3. Discussion

Intratympanic membrane cholesteatoma was first described in 1863 by Hinton [2]. In 1936, Teed reported five cases of congenital cholesteatomas at the TM [3]. In 1977, Smith and Moran reported three cases of tympanic membrane cholesteatomas in children without otorrhea or otologic surgery, but with episodes of acute otitis media [4]. Furthermore, in 1980, Sobol et al. reported a series of 15 cases of intramembranous and mesotympanic cholesteatomas in children [5]. Thirteen of these 15 cases had a history of recurrent otitis media. Intratympanic membrane congenital cholesteatomas are extremely rare and there are only a few previously documented cases. In 2001, Pasanisi et al. described two further cases of intratympanic cholesteatomas in children without a history of otitis media, otorrhea, ear trauma or otologic surgery [6], however, each case had a small mass in the TM.

The development of intratympanic membrane cholesteatoma can cause several complications such as ossicular involvement and subsequent hearing conduction impairment similar to any other cholesteatoma of the middle ear. However, particularly in children, patients with intratympanic membrane cholesteatoma have no initial complaint of hearing loss. Computed tomography is of great importance in assessing the ossicles and middle ear space invasion, because a small pearl on a TM may be the manifestation of a small part of a cholesteatoma in the middle ear cavity. This information influences management plans. Although our second case appeared to have a large mass, the extent of middle ear involvement was not immediately obvious.

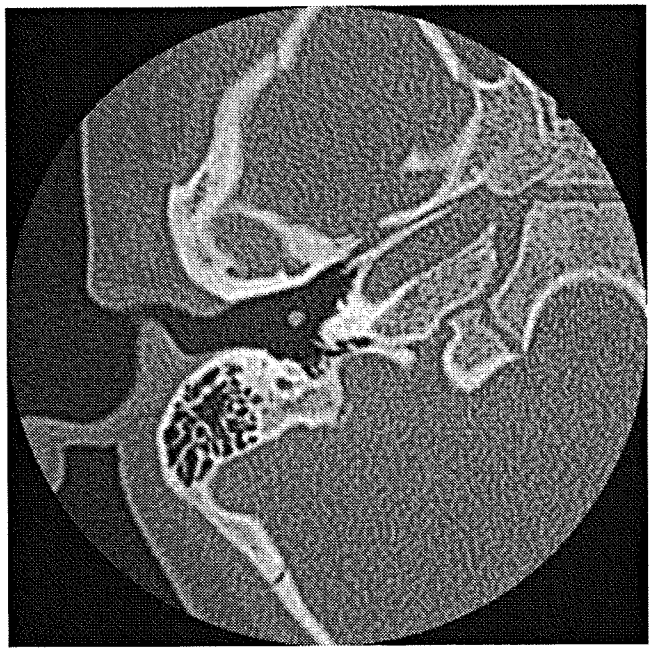

Fig. 2. Axial computed tomography scan of the right temporal bone in Case 1 showing a small soft tissue mass, 2.5 mm in diameter, centered on the umbo of the tympanic membrane.

Fig. 4. Axial computed tomography scan of the right temporal bone of Case 2 showing a large soft tissue mass in the right external auditory canal and the middle ear cavity.

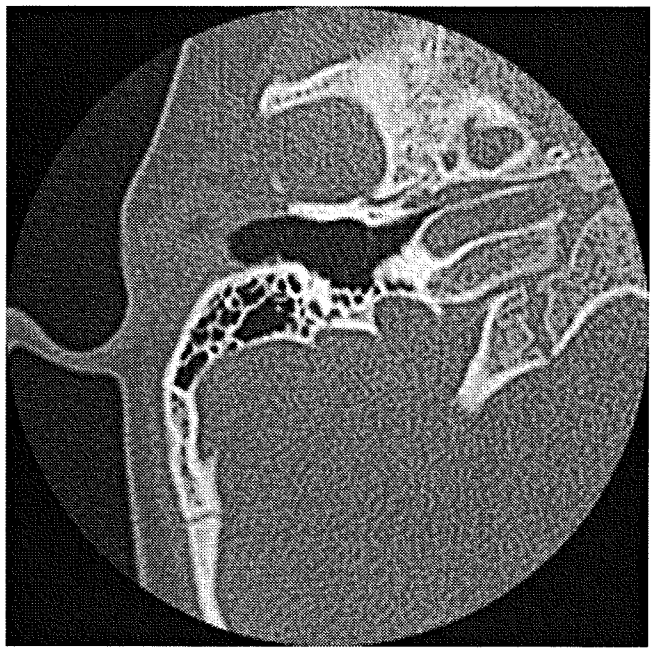

Fig. 5. Three months after surgery with an endaural approach, an axial computed tomography scan of the right temporal bone in Case 2 shows the tympanic membrane in the right place and not showing any mass in the middle ear space.

There are multiple theories regarding the formation of congenital cholesteatomas in the middle ear. The origin of an intratympanic membrane cholesteatoma may be best explained by Sobol et al. They theorized that repeated bouts of middle ear infection stimulate active basal cell ingrowth and proliferation of tympanic membrane epithelium and then proliferated prickle cells coalesce into an intramembranous keratoma [5,7,8]. Our patients differ from this theory by absence of inflammation or disease in the middle ear. The intratympanic membrane cholesteatomas in our cases might have eventually violated the middle ear.

The surgical approach to cholesteatoma of the TM is best treatment, as small intratympanic membrane cholesteatomas, as in our first case, may enlarge, and as shown in our second case, an intratympanic membrane cholesteatoma may compress the fibrous layer of the membrane to the promontory. An endaural approach is recommended to remove the localized cholesteatoma, if the cholesteatoma can be peeled off the TM while maintain an intact fibrous layer of the TM. If a cholesteatoma extends into the middle ear, a tympanoplasty or more extensive approach is necessary to completely remove all the tissue. Recurrence of intratympanic congenital cholesteatoma seems to be less than that for middle ear cholesteatoma [5], however, postoperative follow-up is necessary, especially in cases of large intratympanic membrane cholesteatoma.

4. Conclusion

Our two cases of intratympanic membrane congenital cholesteatomas demonstrate clearly that the development of these lesions can be silent in children. Careful otomicroscopic examination is necessary even in children with no ear symptoms to detect the disease early before it develops beyond the TM.

References

[1] C.E. Reddy, P. Goodyear, S. Ghosh, T. Lesser, Intratympanic membrane cholesteatoma: a rare incidental finding, Eur. Arch. Otorhinolaryngol. 263 (2006) 1061–1064.
[2] J. Hinton, Sebaceous tumor within the tympanum originating on the external surface of the membrane tympani, Guy's Hosp. Rep. 9 (1863) 264.
[3] R. Teed, Cholesteatoma verum tympani: its relationship to the first epibranchial placode, Arch. Otolaryngol. 24 (1936) 455–474.
[4] R. Smith, W.B. Moran, Tympanic membrane keratoma (cholesteatoma) in children with no prior otologic surgery, Laryngoscope 87 (1977) 237–245.
[5] S.M. Sobol, T.J. Reichert, K.D. Faw, M.H. Stroud, G.J. Spector, J.H. Ogura, Intramembranous and mesotympanic cholesteatomas associated with an intact tympanic membrane in children, Ann. Otol. Rhinol. Laryngol. 89 (1980) 312–317.
[6] E. Pasanisi, A. Bacciu, V. Vincenti, S. Bacciu, Congenital cholesteatoma of the tympanic membrane, Int. J. Pediatr. Otorhinolaryngol. 61 (2001) 167–171.
[7] L. Reudi, Pathogenesis and treatment of cholesteatoma in chronic suppuration of temporal bone, Ann. Otol. Rhinol. Laryngol. 66 (1957) 283–305.
[8] L. Reudi, Cholesteatoma formation in the middle ear in animal experiments, Acta Otolaryngol. (Stockh.) 50 (1959) 233–242.

The Laryngoscope

Endothelin-1 Gene Polymorphism and Hearing Impairment in Elderly Japanese

Yasue Uchida, MD, PhD; Saiko Sugiura, MD PhD; Tsutomu Nakashima, MD, PhD; Fujiko Ando, MD, PhD; Hiroshi Shimokata, MD, PhD

Objectives/Hypothesis: To investigate the association between the Lys198Asn (G/T) polymorphism (rs5370) in the endothelin-1 gene (EDN1) and hearing impairment in middle-aged and elderly Japanese.

Study Design: Longitudinal study.

Methods: Data were collected from community-dwelling Japanese adults who participated in the Longitudinal Study of Aging biennially between 1997 and 2006. The participants at baseline were 2,231 adults aged 40 years to 79 years. An average hearing threshold level of 25 dB or better in the better ear for frequencies 500 Hz, 1,000 Hz, 2,000 Hz, and 4,000 Hz was defined as no hearing impairment. Using generalized estimating equations to treat repeated observations within subjects, 7,097 cumulative data were analyzed to assess the association between hearing status and the EDN1 G/T polymorphism with adjustment for age, sex, histories of ear disease, occupational noise exposure, heart disease, hypertension, and body mass index under additive, dominant, and recessive genetic models.

Results: Comparison with wild-type homozygotes (GG), heterozygotes, and mutant homozygotes (GT/TT) showed a positive association with hearing impairment after adjustment for age in model 1 (odds ratio [OR] = 1.24; 95% confidence interval [CI] = 1.02–1.50; $P = .033$), for age and sex in model 2 (OR = 1.29; CI = 1.06–1.57; $P = .0122$), and for age, sex, history of ear disease, and history of occupational noise exposure in model 3 (OR = 1.31; CI = 1.07–1.60; $P = .0092$). The association was also significant in model 3 under the additive model.

Conclusions: This study demonstrated that mutant T-allele carriers were associated with a higher risk of hearing impairment than carriers of wild-type homozygotes in middle-aged and elderly people. This result implies that endothelin-1 plays a valuable role in the cochlea.

Key Words: Endothelin-1, polymorphism, hearing impairment, aging, longitudinal study.

***Laryngoscope*, 119:938–943, 2009**

INTRODUCTION

Presbycusis, which is the general term applied to age-related hearing loss, is a widespread but underrecognized health problem in the elderly population. Presbycusis has been deemed a multifactorial disease. There are many etiological risk factors that cause hearing loss and might contribute to age-related changes in hearing; these include noise exposure, genetic predisposition, ear-related diseases, ototoxic medication, systemic diseases such as cardiovascular disease or diabetes mellitus, socioeconomic status, and lifestyle factors. Studying an outbred and older human population that includes intrinsic and environmental variables accumulated over the course of a lifetime is not easy. Therefore, most studies have identified age-related hearing loss genes using mouse models in a laboratory setting, where rigorous genetic and experimental control can be achieved such that age is the most significant factor in such animal models of age-related hearing loss.[1] To the best of our knowledge, there have been no recent epidemiological studies on common sequence variants that may have a small to moderate phenotypic effect on age-related hearing loss.

Endothelin is a potent vasoactive peptide that is synthesized and released by the vascular endothelium and is a marker of endothelial function. The best-characterized endothelin, endothelin-1, is encoded by a discrete genetic locus on human chromosome 6p24-p23. Once released, its actions are diverse, including vasoactivity,[2] the promotion of mitogenesis/hypertrophy of vascular myocytes,[3,4] profibrotic activity,[5] and the regulation of angiogenesis.[6] Although endothelin-1 was initially thought to be expressed in endothelial cells and to modulate blood flow, later studies showed that it is widely

From the Department of Otorhinolaryngology, National Center for Geriatrics and Gerontology, Obu, Japan (Y.U., S.S.); and Department of Otorhinolaryngology Cognitive and Speech Medicine, Nagoya University School of Medicine, Nagoya, Japan (T.N.), Department of Epidemiology, National Center for Geriatrics and Gerontology, Obu city, Aichi prefecture, Japan (F.A., H.S.).

Editor's Note: This Manuscript was accepted for publication September 3, 2008.

This study was partially supported by a Grant-in-Aid for Comprehensive Research on Aging and Health, from the Ministry of Health, Labor and Welfare of Japan (H17-choju-ippan-033).

Send correspondence to Yasue Uchida, Department of Otorhinolaryngology, National Center for Geriatrics and Gerontology, 36-3 Gengo, Morioka, Obu, Aichi, 474-8511, Japan. E-mail: yasueu@ncgg.go.jp

DOI: 10.1002/lary.20181

distributed in the cardiovascular and noncardiovascular systems,[7] and also distributed in the endolymphatic sac, vestibule, stria vascularis, and spiral ganglion cells of the inner ear.[8–10] This distribution strongly suggests that endothelin-1 must play some meaningful role in the inner ear, but no details are currently known. There have been no previous trials to demonstrate the effect of the endothelin-1 gene (EDN1) polymorphism on hearing impairment. In the present study, we investigated whether a common genetic nonsynonymous variation, an amino acid substitution (lysine/asparagine) at codon 198 (rs5370) of the EDN1 is associated with hearing impairment in a Japanese community-living population of middle and advanced age.

MATERIALS AND METHODS

Subjects

Data for this study were collected from the National Institute for Longevity Sciences –Longitudinal Study of Aging (NILS-LSA), an ongoing population-based study with a 2-year follow-up. The first wave of NILS-LSA examinations was begun in 1997. The participants were independent residents of Aichi Prefecture in central Japan, who were randomly selected from a register stratified by both age and gender in cooperation with the local government. The numbers of men and women recruited were similar, and age at baseline was 40 years to 79 years, with similar numbers of participants in each decade of age (40s, 50s, 60s, and 70s). The study consisted of various gerontological and geriatric measurements, such as medical examinations, blood chemical analysis, body composition, anthropometry, physical function, nutritional analysis, psychological tests, and visual and auditory function.[11] The details of the NILS-LSA have been described elsewhere.[12] The study protocol was approved by the Committee of Ethics of Human Research of the National Center for Geriatrics and Gerontology. Written informed consent was obtained from all subjects. Venous blood samples collected in the first wave of examinations were used for the present genetic analysis. Sera and DNA samples were stored in deep freezers for later examination. With respect to DNA analysis, a number of genotypes related to geriatric diseases, such as Alzheimer's disease, arteriosclerosis, osteoporosis, benign prostate hypertrophy, and diabetes mellitus were examined with the agreement of the participants.

Because the results of both EDN1 genetic analysis and hearing tests were necessary for the present analysis, participation in the first wave of examinations (baseline) was the basic requirement for subject selection. Those who did not allow blood to be drawn or who refused or did not complete the hearing test were excluded. The participants at baseline with results of both EDN1 genetic analysis and a hearing test were 2,231 adults aged 40 years to 79 years. Of these 2,231 baseline participants, 1,788 (80.1%) took part in the second-wave examination, 1,609 (72.1%) were involved in the third-wave examination, and 1,469 (65.8%) participated in the fourth-wave examination. The mean number of repetitive visits was 3.2. The gross accumulation number of participants, regardless of repetitive visits, was 7,097 adults 40 years to 86 years of age who took part in the NILS-LSA between November 1997 (the first wave) and July 2006 (the fourth wave).

The participants filled out detailed questionnaires in advance of the examination visit. The questionnaires consisted of more than 130 items designed to obtain demographic characteristics, personal history, family history, lifestyle habits, and information on various medical problems. Histories of ear disease and occupational noise exposure were obtained in the self-reported account. Histories of heart disease and hypertension were also taken from the self-reported account. Participants who reported either suffering from any ear disease at any time in their life or uncertainty about whether they had suffered from an ear disease were grouped together. History of ear disease was added as a binary variable (yes = 1, no = 0). Occupational noise was defined in the questionnaires as background noise in a work environment over which the worker could not hold a conversation in a normal voice. Former and current noise exposures were combined, and a history of occupational noise exposure was added as the other binary variable (yes = 1, no = 0). Histories of heart disease and hypertension were added as the additional binary variables (presence of the disease = 1, absence = 0). Cases with past or ongoing treatment and with being untreated were combined. Body mass index (BMI) was calculated as weight (in kilograms) divided by height (in meters) squared.

Genetic Analyses

DNA samples were isolated from peripheral blood cells. Genotypes were determined using an allele-specific primer/polymerase chain reaction (PCR) assay system (Toyobo Gene Analysis, Tsuruga, Japan). Genotypes were also determined in control blood known to be from subjects homozygous for the wild-type genotype and heterozygous and homozygous for each variant genotype. The single-nucleotide polymorphism in the EDN1 investigated in the present study was a G-to-T transversion in exon 5 that causes Lys-to-Asn substitution at codon 198.

To determine the EDN1 genotype, the polymorphic region of the gene was amplified by PCR with allele-specific sense primers labeled at the 5′ end either with fluorescein isothiocyanate (FITC) (5′-CCAAGCTGAAAGGCAXGC-3′) or with Texas Red (5′-CCCAAGCTGAAAGGCAXTC-3′) and with an antisense primer labeled at the 5′ end with biotin (5′-TCACATAACGCTCTCTGGAGG-3′). The reaction mixture (25 μL) contained 20 ng of DNA, 5 pmol of each primer, 0.2 mmol/L of each deoxynucleoside triphosphate, 2.0 mmol/L $MgCl_2$, and 1 U of rTaq DNA polymerase (Toyobo, Osaka, Japan) in the appropriate DNA polymerase buffer. The amplification protocol consisted of initial denaturation at 95°C for 5 minutes, 35 cycles of denaturation at 95°C for 30 seconds, annealing at 60°C for 30 seconds, extension at 72°C for 30 seconds, and a final extension at 72°C for 2 minutes.

To determine the EDN1 genotype, amplified DNA was incubated in a solution containing streptavidin-conjugated magnetic beads in the wells of a 96-well plate at room temperature. The plate was placed on a magnetic stand, and the supernatants were then collected from each well, transferred to the wells of a 96-well plate containing 0.01 mol/L NaOH, and measured for fluorescence with a microplate reader (Spectra Fluor; Tecan Co., Tokyo, Japan) at excitation and emission wavelengths of 485 and 538 nm, respectively, for FITC, and of 584 and 612 nm, respectively, for Texas Red.

Auditory Test Procedures

Air-conduction pure-tone thresholds at octave intervals from 125 Hz to 8,000 Hz were obtained using the test method recommended by the Japan Audiological Society, using a diagnostic audiometer (AA-73A and AA-78; Rion, Tokyo, Japan) calibrated according to Japanese Industrial Standards T 1201. Hearing thresholds of the better ear based on a pure-tone average of thresholds at 500 Hz, 1,000 Hz, 2,000 Hz, and 4,000 Hz were used for the present analyses. An average hearing threshold (AHT) level of 25 dB or better for frequencies 500 Hz, 1,000

Hz, 2,000 Hz, and 4,000 Hz was defined as no hearing impairment for the purposes of the present analyses according to the World Health Organization grades.[13]

Statistical Analysis

Statistical analyses were conducted using Statistical Analysis System (SAS) version 9.13 (SAS Institute, Cary, NC). For continuous variables, a *t* test was used to assess differences between two groups and one-way analysis of variance (ANOVA) was used to make comparisons among three groups. Comparisons of categorical variables were performed using the chi-square test. Cumulative data were analyzed using generalized estimating equations (GEEs), which take into account the dependency of repeated observations within subjects; this is an important feature that is necessary for longitudinal analyses. A further advantage of GEEs is that subjects are included regardless of missing values. Thus, subjects who were lost to follow-up after early-wave examination were also included in the analyses. GEE models were fitted by the GENMOD procedure of SAS. The GENMOD procedure fits generalized linear models. The correlation structure was specified to be autoregressive.

The effect of the EDN1 G/T (Lys198Asn) polymorphism on hearing impairment was analyzed using the GENMOD procedure. Genotypes were coded as follows: wild-type homozygotes, GG; heterozygotes, GT; and mutant homozygotes, TT. Because no preceding information regarding the mode of inheritance of the EDN1 G/T polymorphism on hearing impairment can be found, we considered different modes of inheritance as follows: the additive per-allele model, the T allele was compared between cases and controls by assigning scores of 0, 1, and 2 to homozygotes for the G allele, heterozygotes, and homozygotes for the T allele, respectively; the dominant model compared genotypes GG versus GT and TT; and the recessive model compared genotype GG and GT versus TT.

Analyses were carried out with several adjusted models, adjusting for different combinations of confounding variables: age was taken as moderator variable in model 1, age and sex in model 2, and histories of ear disease and occupational noise exposure in addition to age and sex in model 3. Histories of heart disease and hypertension were added in model 4 to moderator variables of model 3, and additionally BMI was included in model 5.

The estimated prevalence of hearing impairment by a dominant genetic model at ages 50 years and 75 years was analyzed assuming that the subject was male, with no occupational noise exposure, and with no history of ear disease.

RESULTS

Table I presents the clinical characteristics of the participants at baseline according to hearing impairment status. The prevalence of hearing impairment was 20.6%. As expected, the subjects with hearing impairment were significantly older and included a higher ratio of males than those without hearing impairment. The characteristics of participants according to EDN1 genotype are shown in Table II. Baseline data were put in the upper panel with *P* value in the rightmost column tested by the ANOVA or chi-square test, and cumulative data were set in the lower panel. The frequencies of the GG, GT, and TT genotypes in the samples at baseline were 52.6%, 40.0%, and 7.4%, respectively. The allele frequencies were 72.6% and 27.4% for the G and T alleles, respectively. These results were not significantly different from those expected based on the Hardy-Weinberg equilibrium (chi-square test, $P > .05$). No value of baseline characteristics, including mean AHT, prevalence of hearing impairment (percentage), sex distribution, and mean age was significantly different among the three genotype groups. The frequencies of the GG, GT, and TT genotypes in the cumulative samples were 53.1%, 39.3%, and 7.6%, respectively.

The results from the GEEs, adjusting for the effects of repeated observations within subjects and confounding factors (age, sex, histories of ear disease, and occupational noise exposure), are presented in Table III. Because the results of model 4 and model 5 were virtually identical to those of model 3 after being rounded to two decimal places, they were not shown in Table III. The genes were analyzed under additive, dominant, and recessive genetic models. Under the additive model of inheritance, a risk for hearing impairment altered by adjustment. The association of the EDN1 G/T polymorphism with hearing impairment was significant in model 3 under the additive model and in all models under the dominant model. The association was significant after adjustment for age in model 1 ($P = .033$), for age and sex in model 2 ($P = .0122$), and for age, sex, history of ear disease, and history of occupational noise exposure in model 3 ($P = .0092$). The odds ratio of hearing impairment in GT/TT subjects compared to that in GG subjects was 1.24 (95% confidence interval [CI], 1.02–1.50) in model 1, 1.29 (CI, 1.06–1.57) in model 2, and 1.31 (CI, 1.07–1.60) in model 3. However, no significant association of the EDN1 G/T polymorphism with hearing impairment was observed in the recessive model ($P > .05$).

The estimated prevalence of hearing impairment by the dominant model at ages 50 years and 75 years were 3.7% (CI, 2.8–4.7) for GG, and 4.7% (CI, 3.6–6.1) for GT/TT at age 50 years, and 58.2% (CI, 53.5–62.7) for GG, and 64.5% (CI, 59.7–69.0) for GT/TT at age 75 years.

DISCUSSION

Many attempts have been made from different perspectives to determine genetic contributions to age-related hearing loss. In the Framingham cohort, the heritability of presbycusis phenotypes was estimated to be 0.35 to 0.55, based on evaluations of audiometric examinations comparing genetically unrelated people (spouse pairs) with genetically related people (sibling pairs, parent-child pairs).[14] According to genome-wide linkage analysis in the Framingham study, the heritability (the proportion of variance due to genes) of age-adjusted pure-tone average at medium and low frequencies was estimated to be 0.38 and 0.31, respectively.[15] Wingfield et al. tested the hearing acuity of monozygotic and dizygotic twin pairs, and reported that approximately two-thirds of the variance in hearing acuity for individuals' better ears in the middle and high frequency ranges could be accounted for by genetic factors.[16] To the best of our knowledge, the present report is the first to examine common genetic variation that contributes to hearing impairment and that stems from a number of genotypes

TABLE I.
Characteristics of Subjects at Baseline According to Hearing Impairment Status.

	No Hearing Impairment	Hearing Impairment	All	*P*
No.	1,772 (79.4%)	459 (20.6%)	2,231	
Sex, % male	47.1	62.5*	50.3	<.0001
Age ± SE, y	56.7 ± 0.2	69.1 ± 0.5*	59.2 ± 0.2	<.0001
AHT ± SE	12.5 ± 0.2	36.4 ± 0.3*	17.4 ± 0.3	<.0001

SE = standard error; AHT = average hearing threshold level for frequencies 0.5, 1, 2, and 4 kHz for the better ear.
*P value tested by t test or χ^2 test.

related to geriatric diseases. Across all ages, environmental and hereditary factors are important sources of variation, with environmental factors becoming more influential with increasing age. Wingfield et al. found that, in cases of asymmetric acuity, the better ear provides a better approximation of what heritability would be prior to the impact of environmental insults.[16] Therefore, hearing thresholds of the better ear based on average pure-tone thresholds were used throughout the present analyses.

In community-dwelling middle-aged and elderly people, we found a significant effect of G/T polymorphism in EDN1 on hearing impairment. The frequencies of the EDN1 genotypes and alleles in the present cohort were similar to those in a previous report on Japanese subjects,[17] and were not significantly different from those in Caucasians.[18] The present results suggest that carriers of the mutant allele (T) experience a dominant effect that manifests itself as an increase in the prevalence of hearing impairment in people past middle age in comparison with carriers of the wild-type homozygote (GG). In other words, an amino acid substitution (Lys/Asn) at codon 198 (rs5370) in EDN1 was significantly associated with hearing impairment. This minor Asn-allele (GT/TT) was associated with a 31% higher risk of hearing impairment than homozygotes with 198Lys (GG) after adjustment for age, sex, history of ear disease, and history of occupational noise exposure in the middle-aged and elderly.

Recent research has shed some light on the connection between endothelin-1 and the cochlea. Experimentally, vasospasm of the spiral modiolar artery (SMA) has been shown to be caused by endothelin-1, which induces a strong, long-lasting constriction of the SMA by increasing contractile apparatus Ca2+ sensitivity via Rho-kinase. Vasospasm of the SMA may cause ischemic stroke of the inner ear, because its blood supply depends exclusively on the SMA, which is a functional end artery.[19,20]

Furthermore, under hypoxic conditions, a clear increase of endothelin-1 activity is induced, potentially leading to vasoconstriction in the stria vascularis. Accordingly, the endocochlear potential may be affected.[21]

On the other hand, it has been demonstrated in previous studies that endothelin-1 is distributed in the central and peripheral nervous systems.[7,22] Endothelin-1 is widely distributed in spiral ganglion cells in the guinea pig and may play a role in auditory transmission. Spiral ganglion neurons are the primary sensory neurons which provide afferent innervation to cochlear hair cells and convey nerve impulses from the cochlear hair cells to the central nervous system. Thus, a better understanding of the characteristics of spiral ganglion cells and their neurotransmission functions will provide insights into the mechanisms of hearing impairment. Endothelin-1 in spiral ganglion cells may have a direct influence on the transmission of nerve impulses.[10]

TABLE II.
Characteristics of Participants According to Endothelin-1 Genotype.

	Genotype			
	GG	GT	TT	*P*
Baseline data				
No.	1,173 (52.6%)	892 (40.0%)	166 (7.4%)	
AHT, mean ± SE	17.0 ± 0.4	18.0 ± 0.4	16.9 ± 1.0	NS
Hearing impairment, %	19.4	22.8	16.9	NS
Sex, % male	51.8	47.5	54.8	NS
Age, y, mean ± SE	59.1 ± 0.3	59.4 ± 0.4	58.8 ± 0.8	NS
Cumulative data				
No.	3,771 (53.1%)	2789 (39.3%)	537 (7.6%)	
Sex, % male	52.9	48.8	55.3	
Age, y, mean ± SE	60.7 ± 0.2	61.1 ± 0.2	60.8 ± 0.5	

AHT = average hearing threshold level for frequencies 0.5, 1, 2, and 4 kHz for the better ear; SE = standard error; NS = not significant.
*P value tested by analysis of variance or χ^2 test.

TABLE III.
Odds Ratios of Hearing Impairment by Polymorphisms in EDN1.

Mode of Inheritance	Genotype GG (T=0)	GT (T=1)	TT (T=2)	P
Additive genetic model*				
No.	3,771	2,789	537	
Model 1	1	1.09 (0.99–1.20)/T allele		NS
Model 2	1	1.10 (0.99–1.22)/T allele		NS
Model 3	1	1.13 (1.02–1.25)/T allele		.0240
	GG	GT/TT		
Dominant genetic model				
No.	3,771	3326		
Model 1	1	1.24 (1.02–1.50)		.0330
Model 2	1	1.29 (1.06–1.57)		.0122
Model 3	1	1.31 (1.07–1.60)		.0092
	GG/GT	TT		
Recessive genetic model				
No.	6,560	537		
Model 1	1	0.96 (0.64–1.43)		NS
Model 2	1	0.93 (0.62–1.40)		NS
Model 3	1	0.92 (0.61–1.38)		NS

NS = not significant.
*The additive genetic model assumes that there is a linear gradient in risk between the GG, GT, and TT genotypes (GG genotype base). This is equivalent to a comparison of the T allele versus the G allele. The per-allele odds ratio for hearing impairment risk is shown under the additive genetic model.
Moderator variable: model 1, age; model 2, age and sex; model 3, age, sex, history of ear disease, and history of occupational noise exposure.
Parenthetical reference shows 95% confidence interval.

However, the mechanisms through which endothelin-1 functions in the auditory system remain to be clarified; further detailed investigation on the role of endothelin-1 on auditory function is required.

The diversity of actions of endothelin may be explained by the existence of several types of endothelin receptors with different cellular functions. Endothelins exert their biological effects via two specific cell surface receptor subtypes termed endothelin receptor type A and endothelin receptor type B. Because the stimulation of these different receptors is known to evoke different and sometimes opposite functions, these receptor gene polymorphisms could have profound implications for the role of endothelin on the hearing system. However, receptor gene polymorphisms were not examined in the present study.

For a multifactorial trait, like age-related hearing loss, numbers of coexisting and risk-modifying factors can be taken into account in analyses. Hypertension and cardiovascular disease have been thought to have some relation to hearing loss.[23] Also, a high BMI has been reported to correlate with age-related hearing loss.[24] At the same time, the significant relation between Lys198Asn polymorphism and a risk of coronary artery disease has been shown.[25] In the present analyses, we added BMI and histories of heart disease and hypertension to the other factors (age, sex, histories of ear disease, and occupational noise exposure) as moderator variables, however, the association of the EDN1 G/T polymorphism with hearing impairment did not alter before and after adjustment for BMI and histories of heart disease and hypertension.

A number of gene polymorphisms related to geriatric diseases were examined in the NILS-LSA. There is expected to be some interactive effect on age-related hearing loss between common variants, and environmental and hereditary factors. Further research on this issue is currently underway.

CONCLUSION

The present study demonstrated that there is a significant association between the EDN1 G/T polymorphism and hearing impairment in middle-aged and elderly people after adjustment for age, sex, occupational noise exposure, and history of ear disease. The

mutant Asn allele was found to be associated with a 31% higher risk of hearing impairment than homozygotes with 198Lys after adjustment for confounding variables in the middle-aged and elderly. This result is consistent with the findings from previous laboratory research regarding the presence and medicinal value of endothelin-1 in the cochlea.

BIBLIOGRAPHY

1. Liu XZ, Yan D. Ageing and hearing loss. *J Pathol* 2007;211: 188–197.
2. Schiffrin EL, Deng LY, Sventek P, Day R. Enhanced expression of endothelin-1 gene in resistance arteries in severe human essential hypertension. *J Hypertens* 1997;15:57–63.
3. Li JS, Lariviere R, Schiffrin EL. Effect of a nonselective endothelin antagonist on vascular remodeling in deoxycorticosterone acetate-salt hypertensive rats: evidence for a role of endothelin in vascular hypertrophy. *Hypertension* 1994;24:183–188.
4. Schiffrin EL. Endothelin: potential role in hypertension and vascular hypertrophy. *Hypertension* 1995;25:1135–1143.
5. Kozakova M, Buralli S, Palombo C, et al. Myocardial ultrasonic backscatter in hypertension: relation to aldosterone and endothelin. *Hypertension* 2003;41:230–236.
6. Kopetz ES, Nelson JB, Carducci MA. Endothelin-1 as a target for therapeutic intervention in prostate cancer. *Invest New Drugs* 2002;20:173–182.
7. Naidoo V, Naidoo S, Raidoo DM. Immunolocalisation of endothelin-1 in human brain. *J Chem Neuroanat* 2004; 27:193–200.
8. Xu DY, Tang YD, Liu SX, Liu J. Distribution and significance of the endothelin 1 in the cochlear lateral wall of guinea pig. *J Laryngol Otol* 2007;121:721–724.
9. Jinnouchi K, Tomiyama S, Pawankar R. Distribution of endothelin-1 like activity in the endolymphatic sac of normal guinea pigs. *Acta Otolaryngol* 1995;115:400–404.
10. Xu D, Tang Y, Liu S, Liu J. Expression and significance of endothelin 1 in spiral ganglion cells of guinea pig. *Int J Pediatr Otorhinolaryngol* 2008;72:189–192.
11. Uchida Y, Nakashima T, Ando F, Niino N, Shimokata H. Is there a relevant effect of noise and smoking on hearing? A population-based aging study. *Int J Audiol* 2005;44:86–91.
12. Shimokata H, Ando F, Niino N. A new comprehensive study on aging—the National Institute for Longevity Sciences, Longitudinal Study of Aging (NILS-LSA). *J Epidemiol* 2000;10:S1–S9.
13. World Health Organization. Prevention of blindness and deafness. Grades of hearing impairment. http://www.who.int/pbd/deafness/hearing_impairment_grades/en/.
14. Gates GA, Couropmitree NN, Myers RH. Genetic associations in age-related hearing thresholds. *Arch Otolaryngol Head Neck Surg* 1999;125:654–659.
15. DeStefano AL, Gates GA, Heard-Costa N, Myers RH, Baldwin CT. Genomewide linkage analysis to presbycusis in the Framingham Heart Study. *Arch Otolaryngol Head Neck Surg* 2003;129:285–289.
16. Wingfield A, Panizzon M, Grant MD, et al. A twin-study of genetic contributions to hearing acuity in late middle age. *J Gerontol A Biol Sci Med Sci* 2007;62:1294–1299.
17. Jin JJ, Nakura J, Wu Z, et al. Association of endothelin-1 gene variant with hypertension. *Hypertension* 2003;41: 163–167.
18. Tiret L, Poirier O, Hallet V, et al. The Lys198Asn polymorphism in the endothelin-1 gene is associated with blood pressure in overweight people. *Hypertension* 1999;33: 1169–1174.
19. Scherer EQ, Herzog M, Wangemann P. Endothelin-1-induced vasospasms of spiral modiolar artery are mediated by rho-kinase-induced Ca(2+) sensitization of contractile apparatus and reversed by calcitonin gene-related peptide. *Stroke* 2002;33:2965–2971.
20. Scherer EQ, Arnold W, Wangemann P. Pharmacological reversal of endothelin-1 mediated constriction of the spiral modiolar artery: a potential new treatment for sudden sensorineural hearing loss. *BMC Ear Nose Throat Disord* 2005;5:10.
21. Mazurek B, Haupt H, Georgiewa P, Klapp BF, Reisshauer A. A model of peripherally developing hearing loss and tinnitus based on the role of hypoxia and ischemia. *Med Hypotheses* 2006;67:892–899.
22. Stokely ME, Yorio T, King MA. Endothelin-1 modulates anterograde fast axonal transport in the central nervous system. *J Neurosci Res* 2005;79:598–607.
23. Rosenhall U, Sundh V. Age-related hearing loss and blood pressure. *Noise Health* 2006;8:88–94.
24. Fransen E, Topsakal V, Hendrickx JJ, et al. Occupational noise, smoking, and a high body mass index are risk factors for age-related hearing impairment and moderate alcohol consumption is protective: a European population-based multicenter study. *J Assoc Res Otolaryngol* 2008;9:264–276.
25. Buhler K, Ufer M, Muller-Marbach A, et al. Risk of coronary artery disease as influenced by variants of the human endothelin and endothelin-converting enzyme genes. *Pharmacogenet Genomics* 2007;17:77–83.

Magn Reson Med Sci, Vol. 8, No. 1, pp. 43-46, 2009

CASE REPORT

Endolymphatic Hydrops of the Labyrinth Visualized on Noncontrast MR Imaging: A Case Report

Shinji NAGANAWA[1]*, Michihiko SONE[2], Hironao OTAKE[2], and Tsutomu NAKASHIMA[2]

Departments of [1]Radiology and [2]Otorhinolaryngology, Nagoya University Graduate School of Medicine
65 Tsurumai-cho, Shouwa-ku, Nagoya 466-8550, Japan
(Received September 22, 2008; Accepted October 29, 2008)

We admitted an 11-year-old girl with enlarged endolymphatic duct and sac syndrome to our hospital with severe nausea and vertigo. Three-dimensional constructive interference in steady state (3D-CISS) and fluid-attenuated inversion recovery (3D-FLAIR) images revealed a reflux of proteinous or hemorrhagic fluid into enlarged endolymphatic space in the labyrinth. This is the first imaging report to show endolymphatic hydrops visualized by noncontrast-enhanced MR imaging in a living human patient.

Keywords: ***endolymphatic hydrops, magnetic resonance imaging, temporal bone disease, 3D imaging***

Introduction

Recent studies have reported the visualization of endolymphatic hydrops on magnetic resonance (MR) imaging after intratympanic administration of Gd-DTPA[1-3] or possibly after intravenous administration of high-dose Gd-DTPA[4] in patients with Ménière's disease. However, such visualization by nonenhanced MR imaging has not been reported in living humans.

Case Report

We admitted an 11-year-old girl with hearing deterioration in her right ear and attacks of vertigo to our hospital for severe nausea and vomiting. Since age 2, she had been followed for enlarged endolymphatic duct and sac syndrome (large vestibular aqueduct syndrome). From time to time, she had hearing loss and vertigo attacks and received steroid drip infusion and hyperbaric oxygen therapy. She also had a goiter and was diagnosed with Pendred syndrome based on genetic analysis. On this admission, hearing in her right ear was unmeasurable on the scale and in the left ear was 86.3 dB (average of 500, 1000, and 2000 Hz).

MR imaging obtained one day after admission (Fig. 1A-D) revealed an enlarged endolymphatic duct and sac that showed high signal on 3-dimensional fluid attenuated inversion recovery (3D-FLAIR) and mixed signal on 3D constructive interference in the steady state (3D-CISS) images. On 3D-FLAIR images, the endolymphatic space in the cochlea and vestibule also showed high signal. Conversely, on 3D-CISS images, the signal in the labyrinth was low. These areas were thought to correspond to the reflux of high proteinous or hemorrhagic fluid from the endolymphatic duct and sac. Reference to images from other patients with Ménière's disease obtained after intratympanic injection of Gd-DTPA suggested that these areas were enlarged endolymphatic space (Fig. 1E).

Her nausea and vomiting improved during her 7-day stay in the hospital. On the day she was released, she fell and hit her head on the floor. She then complained of worsening hearing loss in her left ear and worsened nausea and vomiting and returned to the hospital. Six days after this head trauma, she underwent a second MR examination, which revealed increased signal in the basal turn of the left cochlea on 3D-FLAIR that seemed to extend into the perilymphatic space (Fig. 2).

All MR images were obtained on a 3-tesla scanner (Magnetom TRIO, Siemens Medical Solutions, Erlangen, Germany). We performed 3D-CISS imaging (voxel size $0.5 \times 0.5 \times 0.4$ mm) to obtain reference images of the anatomy of the labyrinthine fluid-space. 3D-FLAIR imaging (voxel size $0.7 \times 0.7 \times 0.8$ mm) was performed using a variable flip-angle echo train with an average flip angle of 120 degrees and an echo-train length of 119. The fea-

*Corresponding author, Phone: +81-52-744-2327, Fax: +81-52-744-2335, E-mail: naganawa@med.nagoya-u.ac.jp

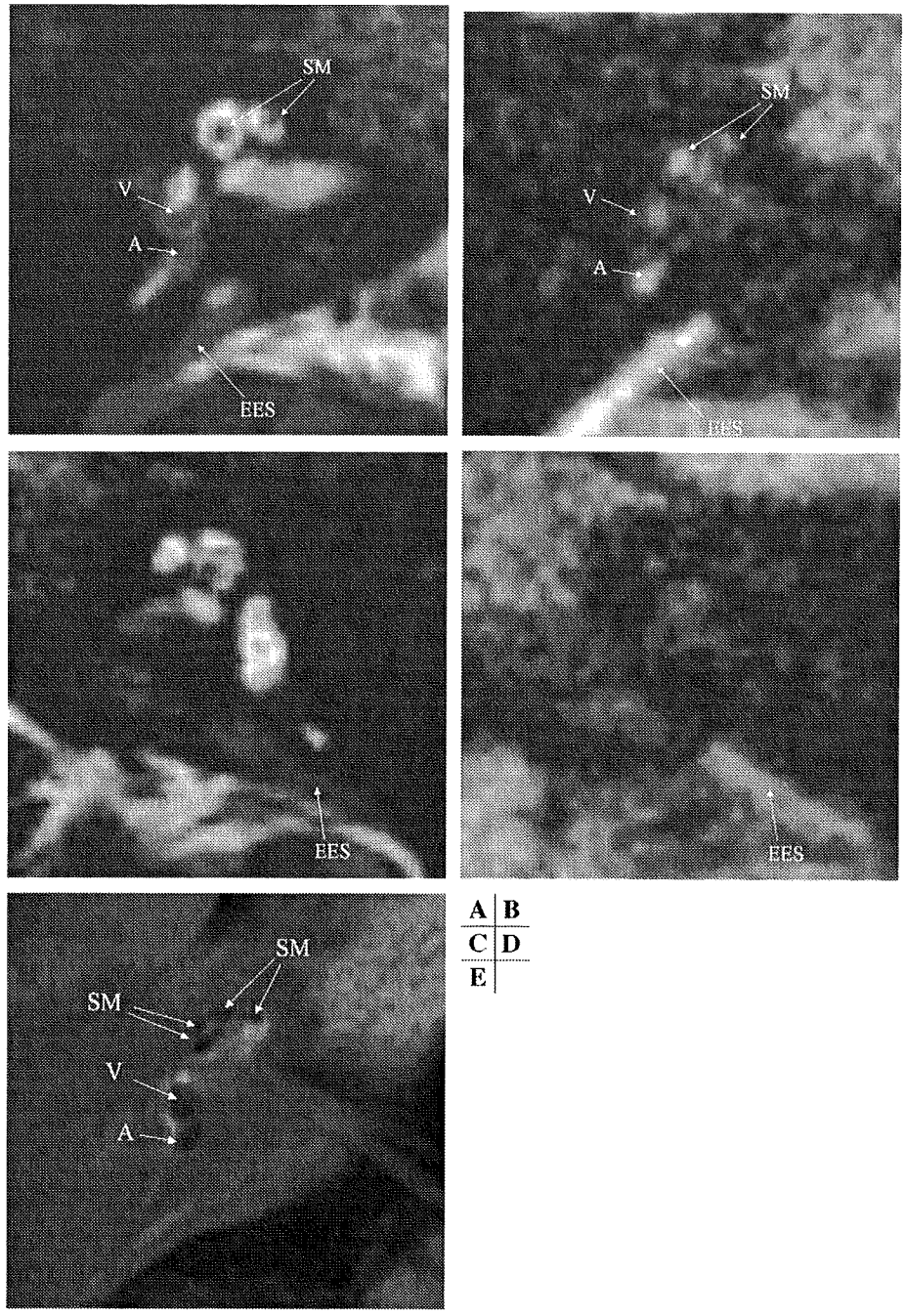

Fig. 1. An 11-year-old girl with bilateral enlarged endolymphatic duct and sac syndrome. First magnetic resonance (MR) imaging series obtained 1 day after admission. (**A**) Posterior part of the enlarged endolymphatic duct and sac of the right ear shows lower signal on the 3-dimensional constructive interference in steady state (3D-CISS) image (arrow; EES). Low signal areas corresponding to endolymphatic space are seen in the cochlea (scala media, SM), vestibule (V), and posterior ampulla (**A**). Conversely, these same areas show high signal on 3D fluid-attenuated inversion recovery (3D-FLAIR) (**B**). Note that no area corresponding to endolymphatic space can be recognized in the left labyrinth on 3D-CISS (**C**) and 3D-FLAIR (**D**). As an anatomical reference for enlarged endolymphatic space, an image from a different patient who had Ménière's disease (a 60-year-old woman) is shown (**E**). This is a 3D real inversion recovery (IR) image acquired after intratympanic injection of Gd-DTPA. This patient does not have an enlarged endolymphatic duct and sac. On 3D real-IR after intratympanic injection of Gd-DTPA, endolymphatic space shows negative signal (black), perilymphatic space shows positive signal (white), and surrounding bone shows zero signal (gray).[2]

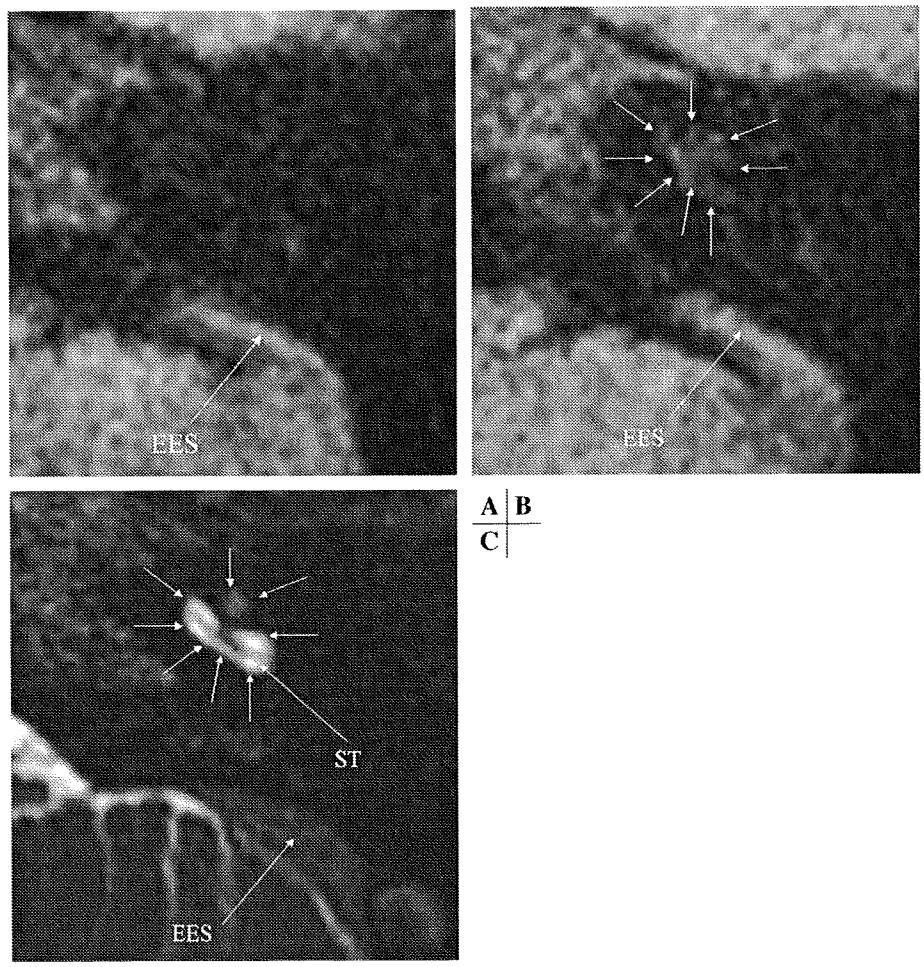

Fig. 2. Images of the left ear. (**A**) A 3-dimensional fluid-attenuated inversion recovery (3D-FLAIR) image from the first magnetic resonance (MR) examination. The enlarged endolymphatic duct and sac show high signal (EES); however, no signal can be detected in the cochlea and vestibule. (**B**) A 3D-FLAIR image from the second MR examination performed 11 days after the first examination and 6 days after minor head trauma after which she experienced worsened left-side hearing loss. The enlarged endolymphatic duct and sac (EES) can be seen as in the previous study, and a slight signal increase can be seen in the cochlea (short arrows). High signal also extended into perilymphatic space. This finding is consistent with the reflux of proteinous or hemorrhagic fluid from the endolymphatic sac into the cochlea and with the contamination of the endo- and perilymph. (**C**) A 3-dimensional constructive interference in steady state (3D-CISS) image from the second MR examination is shown for anatomical reference. On 3D-CISS, the signal of the enlarged endolymphatic sac (EES) is low. That of cochlear fluid (short arrows) is high, suggesting only a small amount of reflux. Comparing (**B**) and (**C**), the high signal in the cochlea in (**B**) can also be seen to extend into the scala tympani (perilymphatic space, ST, C).

tures of this variable flip-angle sequence have been reported elsewhere.[5] This sequence allows the use of very long echo-train lengths without severe blurring while maintaining contrast similar to that of 3D-FLAIR obtained with a conventional turbo spin echo sequence, even with a long effective echo time.

Discussion

Enlarged endolymphatic duct and sac syndrome is the leading cause of progressive sensorineural hearing loss in children and young adults. Though the syndrome is congenital, in most cases, the hearing loss is acquired.[6,7] Because hearing loss increases after minor head trauma, as in our case, patients are usually advised to avoid contact sports.

The cause of hearing loss in this syndrome remains unknown,[8] but 2 major theories exist.[9-12] The first is that cerebrospinal fluid (CSF) pressure in the internal auditory canal is transmitted through an insufficiently developed cochlear modiolus to inner-ear hair cells, but reports of normal-

sized cochlear modioli in some cases of this syndrome[9] seem to refute this theory. The other theory is that the hyperosmolar fluid in the endolymphatic duct and sac refluxes into the labyrinth and damages hair cells.[8] Proteinous or hemorrhagic fluid have been reported in the enlarged endolymphatic duct and sac on MR images.[10] Recent literature supports the latter theory,[9-11] especially a case report of a reflux of proteinous or hemorrhagic fluid from the duct and sac into the labyrinth visualized in 3D-FLAIR images.[11] However, no separate visualization between endo- and perilymph fluid was possible, probably as a result of contamination of the fluid by rupture of the Reissner's membrane.

In the present case, separation between endo- and perilymph was apparent in the right ear, and the endolymphatic space seemed to have enlarged according to the image criteria reported previously.[13] In the criteria, the size of the endolymphatic space in the cochlear basal turn was scored subjectively from 0 to 3: 3, the cochlear duct is larger than the perilymphatic space of the scala vestibule; 2, the Reissner's membrane is bulging toward the scala vestibule but smaller than the perilymphatic space of the scala vestibule; 1, the Reissner's membrane is not bulging; and 0, the Reissner's membrane is bulging toward the scala media or there is no visualization of endolymphatic space. In our patient, the score of the right cochlea was 3. In the left ear, in contrast, contamination of the endo- and perilymph seemed likely at the time of the second MR examination.

This case report provides the first images that show endolymphatic hydrops visualized by non-contrast-enhanced MR imaging in a human patient. It is also the first imaging report to suggest fluid reflux into the cochlea just after head trauma in this syndrome. The knowledge obtained from the present case may improve understanding of the pathophysiology of enlarged endolymphatic duct and sac syndrome.

References

1. Nakashima T, Naganawa S, Sugiura M, et al. Visualization of endolymphatic hydrops in patients with Meniere's disease. Laryngoscope 2007; 117: 415-420.
2. Naganawa S, Satake H, Kawamura M, Fukatsu H, Sone M, Nakashima T. Separate visualization of endolymphatic space, perilymphatic space and bone by a single pulse sequence; 3D-inversion recovery imaging utilizing real reconstruction after intratympanic Gd-DTPA administration at 3 Tesla. Eur Radiol 2008; 18:920-924.
3. Naganawa S, Sugiura M, Kawamura M, Fukatsu H, Sone M, Nakashima T. Imaging of endolymphatic and perilymphatic fluid at 3T after intratympanic administration of gadolinium-diethylenetriamine pentaacetic acid. AJNR Am J Neuroradiol 2008; 29:724-726.
4. Carfrae MJ, Holtzman A, Eames F, Parnes SM, Lupinetti A. 3 Tesla delayed contrast magnetic resonance imaging evaluation of Ménière's disease. Laryngoscope 2008; 118:501-505.
5. Naganawa S, Sugiura M, Kawamura M, Fukatsu H, Nakashima T, Maruyama K. Prompt contrast enhancement of cerebrospinal fluid space in the fundus of the internal auditory canal: observations in patients with meningeal diseases on 3D-FLAIR images at 3 Tesla. Magn Reson Med Sci 2006; 5: 151-155.
6. Mafee MF, Charletta D, Kumar A, Belmont H. Large vestibular aqueduct and congenital sensorineural hearing loss. AJNR Am J Neuroradiol 1992; 13:805-819.
7. Emmett JR. The large vestibular aqueduct syndrome. Am J Otol 1985; 6:387-415.
8. Okamoto K, Ito J, Furusawa T, Sakai K, Horikawa S, Tokiguchi S. MRI of enlarged endolymphatic sacs in the large vestibular aqueduct syndrome. Neuroradiology 1998; 40:167-172.
9. Naganawa S, Ito T, Iwayama E, et al. MR imaging of the cochlear modiolus: area measurement in healthy subjects and in patients with a large endolymphatic duct and sac. Radiology 1999; 213: 819-823.
10. Naganawa S, Koshikawa T, Iwayama E, et al. MR imaging of the enlarged endolymphatic duct and sac syndrome by use of a 3D fast asymmetric spin-echo sequence: volume and signal-intensity measurement of the endolymphatic duct and sac and area measurement of the cochlear modiolus. AJNR Am J Neuroradiol 2000; 21:1664-1669.
11. Sugiura M, Naganawa S, Sato E, Nakashima T. Visualization of a high protein concentration in the cochlea of a patient with a large endolymphatic duct and sac, using three-dimensional fluid-attenuated inversion recovery magnetic resonance imaging. J Laryngol Otol 2006; 120:1084-1086.
12. Lemmerling MM, Mancuso AA, Antonelli PJ, Kubilis PS. Normal modiolus: CT appearance in patients with a large vestibular aqueduct. Radiology 1997; 204:213-219.
13. Naganawa S, Satake H, Iwano S, Fukatsu H, Sone M, Nakashima T. Imaging endolymphatic hydrops at 3 tesla using 3D-FLAIR with intratympanic Gd-DTPA administration. Magn Reson Med Sci 2008; 7:85-91.

Acta Oto-Laryngologica, 2010; 130: 338–343

informa
healthcare

ORIGINAL ARTICLE

Endolymphatic hydrops revealed by intravenous gadolinium injection in patients with Ménière's disease

TSUTOMU NAKASHIMA[1], SHINJI NAGANAWA[2], MASAAKI TERANISHI[1], MITSUHIKO TAGAYA[1], SEIICHI NAKATA[1], MICHIHIKO SONE[1], HIRONAO OTAKE[1], KEN KATO[1], TOMOYUKI IWATA[1] & NAOKI NISHIO[1]

[1]*Department of Otorhinolaryngology and* [2]*Department of Radiology, Nagoya University, Nagoya, Japan*

Abstract

Conclusion: Visualization of endolymphatic hydrops became possible after intravenous gadolinium (Gd) injection in patients with Ménière's disease. *Objective:* To visualize endolymphatic hydrops after intravenous Gd injection. *Methods:* Gd (gadoteridol; 0.2 mmol/kg) was injected intravenously in three patients with unilateral Ménière's disease. We performed three-dimensional fluid attenuated inversion recovery (3D-FLAIR) and three-dimensional real inversion recovery (3D-real IR) magnetic resonance imaging (MRI) 4 h after the injection using a 3-Tesla MRI unit. We used a 32-channel array coil to obtain a high signal-to-noise ratio. *Results:* Endolymphatic hydrops was observed in the ears of patients with Ménière's disease. However, Gd concentration in the perilymph was lower compared with that obtained after intratympanic Gd injection.

Keywords: *FLAIR, MRI, real IR MRI, intravenous gadolinium administration*

Introduction

Endolymphatic hydrops has been visualized after intratympanic gadolinium (Gd) injection using 3-Tesla magnetic resonance imaging (MRI) [1]. Gd enters the perilymphatic space through the round window membrane and can then delineate the perilymphatic and endolymphatic spaces. Three-dimensional fluid attenuated inversion recovery (3D-FLAIR) MRI and three-dimensional real inversion recovery (3D-real IR) MRI allow visualization of the endolymphatic space [2,3]. 3D-real IR MRI is generally better for visualizing the endolymphatic space than 3D-FLAIR MRI. However, when Gd concentration is not sufficient in the perilymph, it is more difficult to visualize the Gd in 3D-real IR MRI than in 3D-FLAIR MRI [4].

Gd is generally administered intravenously for contrast enhancement of MRI. If endolymphatic imaging by intravenous Gd injection becomes readily available, the intravenous method will be used widely [5]. At present, however, the signal-to-noise ratio is still insufficient to clearly demonstrate the endolymphatic space after ordinary intravenous Gd injection [6]. Gd concentration in the perilymph reaches its maximum level 4 h after intravenous administration of the drug [7]. Carfrae et al. [8] performed 3 T MRI 4 h after intravenous injection of a triple dose of Gd in normal subjects and patients with Ménière's disease. However, the resultant images were not convincing [9]. These authors did not perform 3D-FLAIR MRI. In this study, we attempted to visualize the endolymphatic space using 3D-FLAIR and 3D-real IR MRI carried out 4 h after intravenous injection of a double dose of Gd in patients with Ménière's disease.

Material and methods

Patients

Three patients with Ménière's disease were enrolled in this study (Table I). Case 1 was a 60-year-old woman who had had left fluctuating hearing loss

Correspondence: Tsutomu Nakashima, Nagoya University School of Medicine, Department of Otorhinolaryngology, 65, Tsurumai-cho, Showa-ku, Nagoya 466-8550, Japan. E-mail: tsutomun@med.nagoya-u.ac.jp

(Received 24 April 2009; accepted 21 June 2009)

ISSN 0001-6489 print/ISSN 1651-2251 online
DOI: 10.3109/00016480903143986

Table I. Patients' details.

Case no.	Gender	Age (years)	Side	Average hearing level (dB)	Hearing fluctuation	Vertigo attacks	AAO-HNS classification
1	F	60	Right	115	No	Non-rotatory	Possible
			Left	68	Yes		
2	M	41	Right	20	Yes	Rotatory	Definite
			Left	6	No		
3	F	67	Right	62	Yes	Rotatory	Definite
			Left	13	No		

Average hearing level is average (dB) of three frequencies (500, 1000, and 2000 Hz). F, female; M, male.

and dizziness for 10 months. Because she had not experienced definitive episodes of rotatory vertigo, she was diagnosed as having possible Ménière's disease according to the criteria of the 1995 American Academy of Otolaryngology-Head and Neck Surgery (AAO-HNS) [10]. Although she had left otitis media with a large perforation of the tympanic membrane, otorrhea was not recognized. When she was 58 years old, she underwent surgery to remove the right acoustic tumor via the posterior fossa, which was performed by a neurosurgeon. After the surgery, she lost right hearing ability completely. Her left average hearing level of three frequencies (500, 1000, and 2000 Hz) was 68 dB with an air–bone gap of 28 dB at the time she was examined by MRI.

Case 2 was a 41-year-old man with right fluctuating hearing loss. When he was 36 years old, he had low-tone sensorineural hearing loss on the right side without vertigo. Subsequently, he experienced fluctuation of his right hearing level. He had also had vertigo attacks, starting at 39 years of age. He had had three definite episodes of vertigo attacks and many drop attacks. He was diagnosed as having definite Ménière's disease according to the criteria of AAO-HNS. His right average hearing level of three frequencies was 20 dB with low-tone sensorineural hearing loss. The left hearing level was normal.

Case 3 was a 67-year-old woman. She had had four definite episodes of vertigo attacks with fluctuation of her right hearing level for 10 months. She was diagnosed as having definite Ménière's disease according to the criteria of AAO-HNS. Her right average hearing level of three frequencies was 62 dB with flat-type sensorineural hearing loss. The left hearing level was normal.

All patients gave informed consent to participate in this study. Their written informed consent was attached to the electronic medical record. The protocol of this study was approved by the Ethics Review Committee of the Nagoya University School of Medicine (approval number 587-2).

Intravenous Gd injection

Gadoteridol (ProHance®) was injected intravenously. The injected amount was 0.4 ml/kg (0.2 mmol/kg). Although the standard amount of gadoteridol is 0.2 ml/kg, a concentration of 0.4 ml/kg is permitted by the Japanese governmental health insurance system if the aim is to visualize metastatic brain tumors. At 4 h after the intravenous gadoteridol injection, MRI was performed.

MRI

MRI scans were performed with a 3 T MRI unit using a multichannel coil. We started with an 8-channel head coil and then switched to a 12-channel coil; we now use a 32-channel array coil to obtain a high signal-to-noise ratio [6]. Heavily T2-weighted 3D constructive interference in the steady-state imaging was obtained for anatomic reference and 3D-FLAIR was then performed to detect perilymph enhancement, while suppressing the signal from the endolymph. Finally, we obtained 3D-real IR images to visualize the endolymph, perilymph, and bone separately on a single image. The details of the MRI protocol were described previously [1–3]. In this study, the inversion time of the 3D-real IR images was extended up to 2000 ms, to adjust for the lower Gd concentration in the perilymph when compared with that delivered by intratympanic injection.

Results

In case 1, evaluation of endolymphatic space was possible in 3D-FLAIR and 3D-real IR MRI because Gd enhancement of the perilymph was relatively good on both sides. Significant endolymphatic hydrops was observed both in the cochlea and in the vestibule of the left ear (Figure 1). In the right ear, in which the acoustic tumor remained in the internal auditory canal (Figure 2), endolymphatic hydrops was not observed.

In case 2 the Gd enhancement was not as prominent as that observed in case 1. Evaluation of endolymphatic

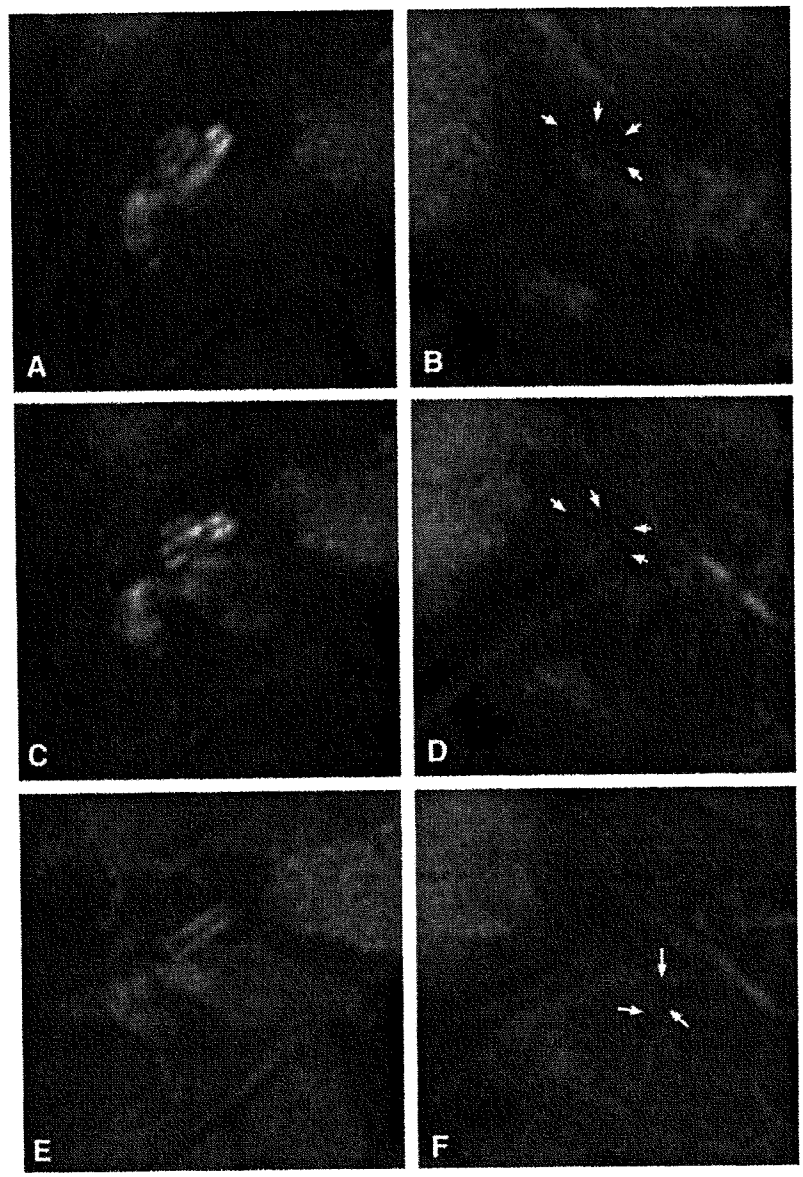

Figure 1. Consecutive sections of 3D-real IR MRI in case 1. A and B, C and D, and E and F are the same sections. A, C, and E show the right ear; B, D, and F show the left ear. Significant endolymphatic hydrops was observed in the left ear. Arrows in B and D indicate endolymphatic hydrops in the cochlea (black areas without Gd). Arrows in F indicate endolymphatic hydrops in the vestibule.

size was difficult in 3D-real IR MRI. However, significant hydrops was observed both in the cochlea and in the vestibule of the right ear in 3D-FLAIR MRI (Figure 3). Gd enhancement was much less evident in the normal left ear than in the right ear. No hydrops was recognized in the left ear.

In case 3, the Gd enhancement was clearer than that in case 2, but weaker than that in case 1. The Gd enhancement was barely recognized in 3D-real IR MRI. However, 3D-real IR MRI helped evaluation of the endolymphatic space size. Significant hydrops was observed both in the cochlea and in the vestibule of the right ear in 3D-FLAIR (Figure 4) and 3D-real IR MRI (Figure 5). Gd enhancement was less evident in the normal left ear than in the right ear. No hydrops was recognized in the left ear.

In all patients, endolymphatic hydrops was observed in the ear with fluctuating hearing loss. Both 3D-FLAIR MRI and 3D-real IR MRI were useful for evaluation of the size of the endolymphatic space.

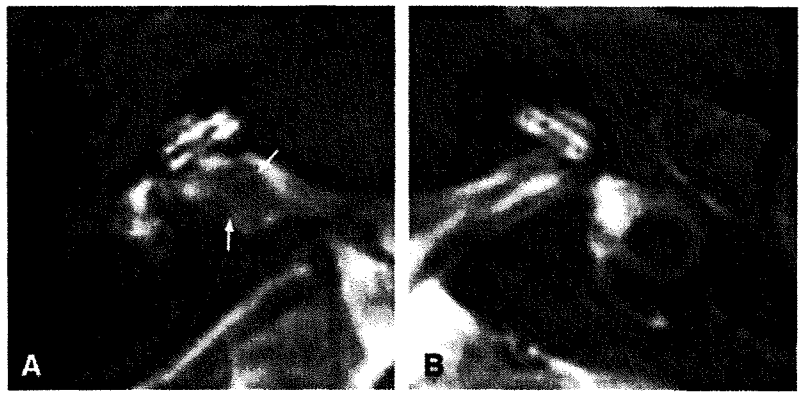

Figure 2. Heavily T2-weighted 3D constructive interference in the steady-state imaging of case 1. A, right ear; B, left ear. In these heavily T2-weighted images, both the endolymph and the perilymph are white and no differences were detected between the right and left ears. The remaining acoustic tumor of the right ear is indicated by arrows.

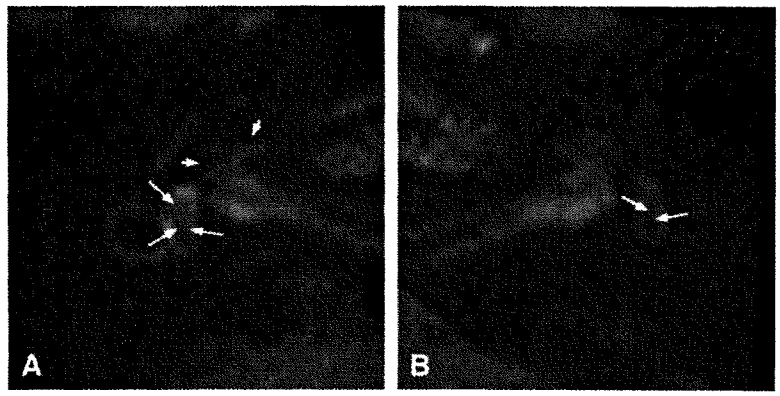

Figure 3. 3D-FLAIR MRI of case 2. A, right ear; B, left ear. In A, short arrows indicate endolymphatic hydrops in the basal turn of the cochlea (wedge-like areas). In 3D-FLAIR MRI, endolymphatic hydrops cannot be discriminated from the surrounding bone. In B, no cochlear hydrops is observed. In A and B, long arrows indicate endolymphatic space in the vestibule. The endolymphatic space is clearly larger in A than in B.

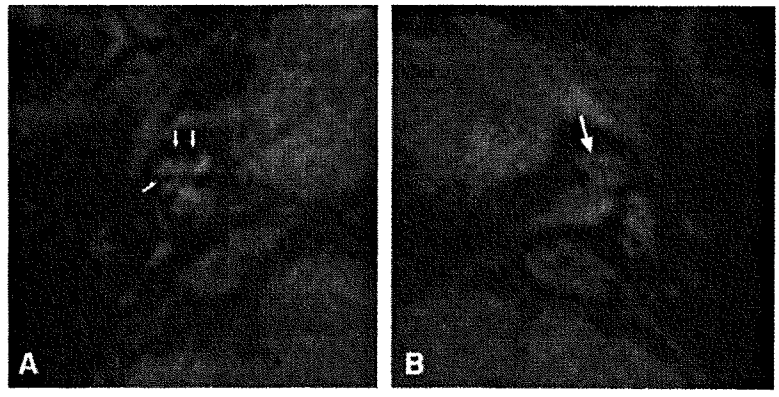

Figure 4. 3D-FLAIR MRI of case 3. A, right ear; B, left ear. In A, short arrows indicate endolymphatic hydrops in th basal and upper turns of the cochlea (wedge-like areas). In B, the cochlea shown by an arrow has no hydrops.

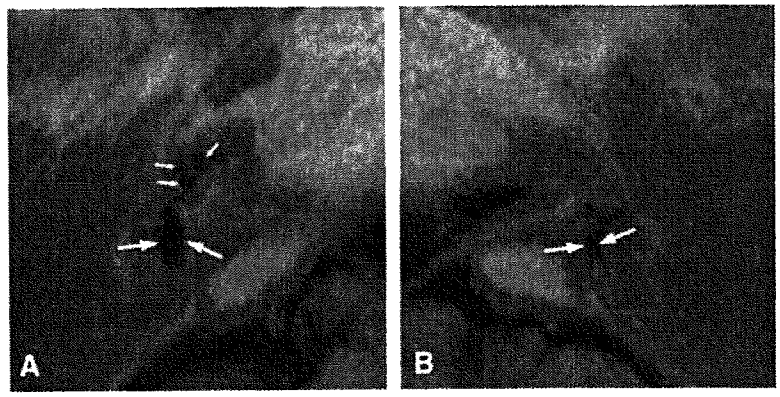

Figure 5. 3D-real IR MRI of case 3. A, right ear; B, left ear. In A, short arrows indicate endolymphatic hydrops in the basal and upper turns of the cochlea (black areas). In A and B, long arrows indicate endolymphatic space in the vestibule. The endolymphatic space is clearly larger in A than in B.

Discussion

We have successfully visualized endolymphatic hydrops after intravenous Gd injection. The blood-labyrinthine barrier includes the blood–endolymph barrier and blood–perilymph barrier. Because the blood–endolymph barrier is extremely tight compared with the blood–perilymph barrier, Gd administered intravenously enters the perilymph but does not enter the endolymph [11]. This difference made it possible to visualize the endolymphatic space of the inner ear in 3D-FLAIR and 3D-real IR MRI after intravenous injection of a double dose of Gd.

The Gd concentration in the perilymph was fainter than that observed after intratympanic injection of Gd diluted 8-fold, and seemed to be closer to the concentration observed after intratympanic injection of Gd diluted 16-fold. We were able to evaluate the degree of endolymphatic hydrops after intratympanic injection of the 16-fold dilution; however, to enhance image contrast, we are now using Gd diluted eightfold as the intratympanic injection method [4].

3D-real IR MRI was generally better than 3D-FLAIR MRI for visualizing the endolymphatic space, as the former discriminated the endolymphatic space not only from the perilymphatic space but also from the surrounding bone [2]. However, low Gd concentrations in the perilymph were more difficult to visualize by 3D-real IR MRI than by 3D-FLAIR MRI [4]. Accordingly, both 3D-FLAIR and 3D-real IR MRI are required for the precise evaluation of the endolymphatic space after intravenous Gd injection.

In case 1, intratympanic Gd injection was not suitable in the left ear because of a large perforation of the tympanic membrane. Intravenous Gd administration was necessary for the image diagnosis of endolymphatic hydrops. The Gd enhancement in the right ear with acoustic tumor was clear. This was probably due to the disrupted blood–labyrinthine barrier in the ear with acoustic tumor. In cases 2 and 3, the Gd enhancement was higher in the ear with Ménière's disease than in the normal ear. We can now evaluate the blood–labyrinthine barrier by intravenous injection of Gd.

Conclusion

We successfully visualized endolymphatic hydrops using 3D-FLAIR and 3D-real IR MRI performed 4 h after intravenous injection of a double dose of Gd, although the quality of the image was not as good as that obtained after intratympanic injection of Gd diluted eightfold with saline. The intravenous administration method, which has high applicability in clinical use, will be used to evaluate the endolymphatic space and the blood–labyrinth barrier on both sides.

This study was supported by research grants from the Ministry of Health, Labour and Welfare in Japan.

References

[1] Nakashima T, Naganawa S, Sugiura M, Teranishi M, Sone M, Hayashi H, et al. Visualization of endolymphatic hydrops in patients with Meniere's disease. Laryngoscope 2007;117:415–20.

[2] Naganawa S, Satake H, Kawamura M, Fukatsu H, Sone M, Nakashima T. Separate visualization of endolymphatic space, perilymphatic space and bone by a single pulse sequence; 3D-inversion recovery imaging utilizing real reconstruction after intratympanic Gd-DTPA administration at 3 Tesla. Eur Radiol 2008;18:920–4.

[3] Naganawa S, Sugiura M, Kawamura M, Fukatsu H, Sone M, Nakashima T. Imaging of endolymphatic and perilymphatic fluid at 3T after intratympanic administration of gadolinium-diethylene-triamine pentaacetic acid. AJNR Am J Neuroradiol 2008;29:724–6.

[4] Nakashima T, Naganawa S, Katayama N, Teranishi M, Nakata S, Sugiura M, et al. Clinical significance of endolymphatic imaging after intratympanic gadolinium injection. Acta Otolaryngol Suppl 2009;560:9–14.
[5] Lane JI, Witte RJ, Bolster B, Bernstein MA, Johnson K, Morris J. State of the art: 3T imaging of the membranous labyrinth. AJNR Am J Neuroradiol 2008;29:1436–40.
[6] Naganawa S, Nakashima T. Cutting edge of inner ear MRI. Acta Otolaryngol Suppl 2009;560:15–21.
[7] Naganawa S, Komada T, Fukatsu H, Ishigaki T, Takizawa O. Observation of contrast enhancement in the cochlear fluid space of healthy subjects using a 3D-FLAIR sequence at 3 Tesla. Eur Radiol 2006;16:733–7.
[8] Carfrae MJ, Holtzman A, Eames F, Parnes SM, Lupinetti A. 3 Tesla delayed contrast magnetic resonance imaging evaluation of Meniere's disease. Laryngoscope 2008;118:501–5.
[9] Naganawa S, Nakashima T. In reference to 3 Tesla delayed contrast magnetic resonance imaging evaluation of Meniere's disease. Laryngoscope 2008;118:1904–5.; author reply 1905.
[10] Committee on Hearing and Equilibrium guidelines for the diagnosis and evaluation of therapy in Meniere's disease. American Academy of Otolaryngology-Head and Neck Foundation, Inc. Otolaryngol Head Neck Surg 1995;113:181–5.
[11] Zou J, Poe D, Bjelke B, Pyykkö. Visualization of inner ear disorders with MRI in vivo: from animal models to human application. Acta Otolaryngol Suppl 2009;560:22–31.

ELSEVIER

Auris Nasus Larynx 37 (2010) 220–222

AURIS NASUS LARYNX
INTERNATIONAL JOURNAL OF ORL & HNS

www.elsevier.com/locate/anl

Changes in endolymphatic hydrops in a patient with Meniere's disease observed using magnetic resonance imaging

Michihiko Sone [a,*], Shinji Naganawa [b], Masaaki Teranishi [a], Seiichi Nakata [a], Naomi Katayama [a], Tsutomu Nakashima [a]

[a] *Department of Otorhinolaryngology, Nagoya University Graduate School of Medicine, 65 Tsurumai-cho, Showa-ku, Nagoya 466-8550, Japan*
[b] *Department of Radiology, Nagoya University Graduate School of Medicine, Nagoya, Japan*

Received 1 December 2008; accepted 16 April 2009
Available online 21 June 2009

Abstract

We describe a case report of a patient with Meniere's disease whose changes in endolymphatic hydrops were observed using magnetic resonance imaging (MRI). Gadolinium was injected intratympanically through the tympanic membrane, and MRI scans performed with a 3-T MRI unit revealed endolymphatic hydrops inside the perilymphatic space filled with gadolinium. We evaluated the relationship between the image findings and hearing level. The correlation between the degree of endolymphatic hydrops observed by MRI and hearing level in patients with Meniere's disease offers a promising new method to study the progression of Meniere's disease.

Keywords: Meniere's disease; Endolymphatic hydrops; Magnetic resonance imaging; Gadolinium; Hearing level

1. Introduction

Endolymphatic hydrops are recognized as the main pathological change of Meniere's disease. Many animal studies and human temporal studies have focused on changes in inner ear function associated with endolymphatic hydrops. Clinically, the severity of endolymphatic hydrops in a patient with Meniere's disease should be estimated in relation to the hearing level, and the results of electrocochleography (EcochG) or vestibular-evoked myogenic potential (VEMP) because pathological examination of the inner ear is not possible.

One report detailed the imaging analysis of the inner ear in patients with Meniere's disease using magnetic resonance imaging (MRI) with intratympanic administration of gadolinium [1]. The clinical imaging of endolymphatic hydrops using 3-T three-dimensional fluid-attenuated inversion recovery (3D-FLAIR) MRI was recently reported [2]. A correlation between the degree of endolymphatic hydrops observed by MRI and clinical symptoms in patients with Meniere's disease offers a promising new method to study the progression of Meniere's disease.

We describe a case report of a patient with Meniere's disease whose changes in endolymphatic hydrops were observed using MRI. We evaluated the relationship between image findings and hearing level.

2. Case report

A 41-year-old man was referred to our department because of Meniere's disease in his left ear, which had begun two years earlier. He had sensorineural hearing loss of 30 dB on the left side. Since the first visit, his hearing level deteriorated gradually so that he experienced rotatory vertigo attacks despite medical treatment, which forced him to close his business for 1 year. During this down period, he received intratympanic gentamicin injection six times in total, and he was able to return to work without experiencing severe vertigo attacks. A caloric test with ice water after gentamicin injection showed no response on the left side.

* Corresponding author. Tel.: +81 52 744 -2323; fax: +81 52 744 2325.
E-mail address: michsone@med.nagoya-u.ac.jp (M. Sone).

0385-8146/$ – see front matter © 2009 Elsevier Ireland Ltd. All rights reserved.
doi:10.1016/j.anl.2009.04.013

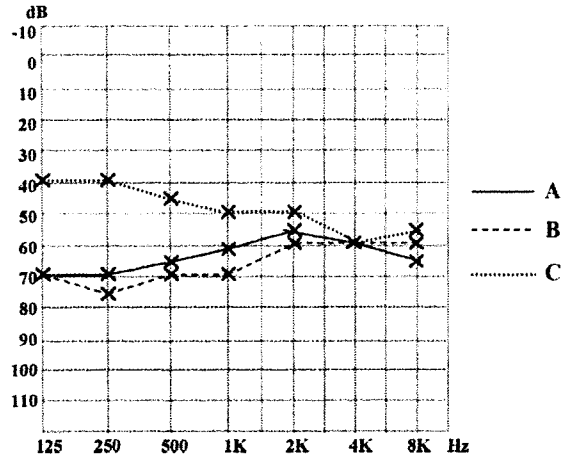

Fig. 1. Hearing levels on pure tone audiometry at the time of the initial (A), second (B), and third (C) magnetic resonance image examinations.

Two years after the treatment, the patient complained of frequent drop attacks. His hearing level at that time was 55–70 dB (Fig. 1A). A VEMP test and EcochG were performed at this time. Surface myogenic potentials in the sternocleidomastoid muscle were added 150 times with a reference electrode over the sternum while clicks (105 dB) were presented to the ipsilateral ear and white noise (75 dB) was presented to the contralateral ear (Synax 2100, NEC Medical Systems, Tokyo, Japan). EcochG was performed with a silver ball electrode placed on the posteroinferior quadrant of the external ear canal, close to the tympanic membrane. The click stimuli were presented four times a second with rarefaction and condensation polarity (Synax 2100). The signal was added 500 times through the bandpass filter (100–3000 Hz). VEMP was absent, and the SP/AP ratio on EcochG was 48%.

To investigate the patient's inner ear condition more completely, gadodiamide hydrate (Omniscan®, Daiich Pharmaceutical Co. Ltd, Tokyo, Japan) diluted eightfold with saline was injected intratympanically through the tympanic membrane, and MRI scans were performed with a 3-T MRI unit (Trio, Siemens, Erlangen, Germany) 24 h after the injection [2]. The patient gave written informed consent to participate in this MRI examination in accordance with the suggestion of the Ethics Review Committee.

3D-FLAIR MRI revealed significant endolymphatic hydrops inside the perilymphatic space filled with gadolinium, which was observed in the lower and upper turns of the cochlea (Fig. 2A) [3]. The gadolinium was faintly visible in the vestibule and the lateral semicircular canal. Seven months after the first gadolinium injection, his hearing level recovered to 45 dB without drop attacks, and a second MRI examination with gadolinium injection was planned. However, a few weeks before the second examination, his hearing level began to deteriorate to 60–75 dB, especially at lower frequencies

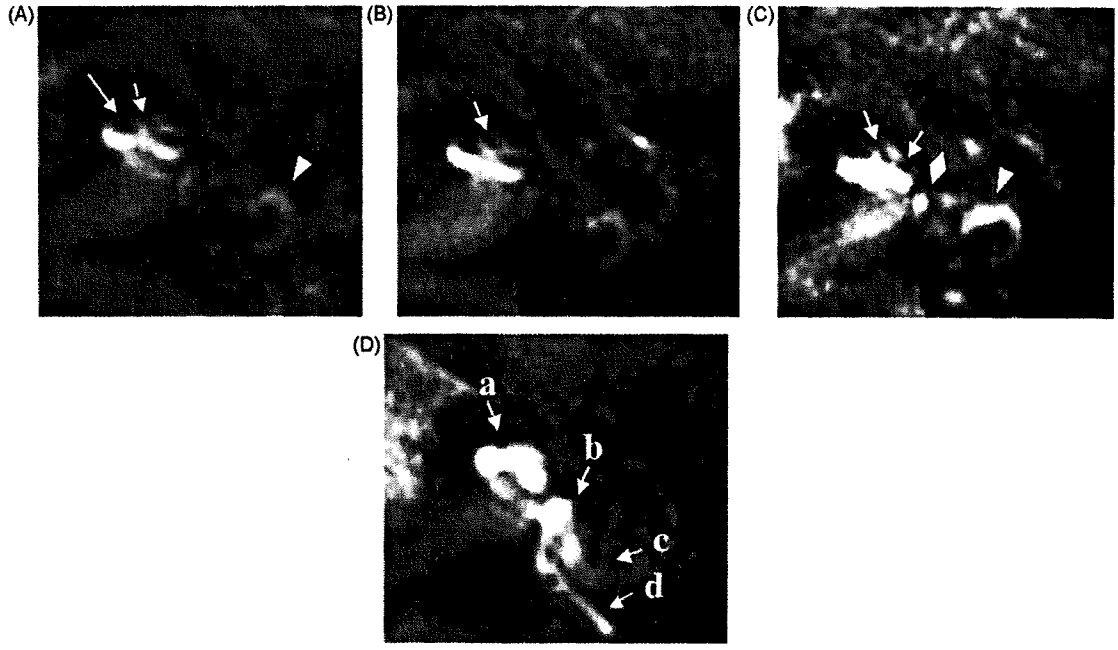

Fig. 2. Three-dimensional fluid-attenuated inversion recovery magnetic resonance images on the axial plane. (A) The initial image shows endolymphatic space inside the perilymphatic space filled with the gadolinium in the lower (long arrow) and upper (short arrow) turns of the cochlea, and faintly visible gadolinium in the lateral semicircular canal (arrowhead). (B) The image at the second examination shows endolymphatic hydrops to a similar degree as that observed in the first MRI, and the hydrops in the upper turn of the cochlea is obvious (short arrow). (C) The image at the third examination shows reduced endolymphatic space in the cochlea (short arrows) and more strongly visible gadolinium in the vestibule (diamond) and the semicircular canal (arrowhead). (D) An image from a patient with acute sensorineural hearing loss with no endolymphatic hydrops is given as an example for comparison. (a) The cochlea, (b) the vestibule, and (c) the lateral and (d) posterior semicircular canals. The endolymphatic space is not clearly visible in this case.